On the role of human sensorimotor feedforward and feedback control in a trajectory tracking task

Momona Yamagami * **Darrin Howell** * **Eatai Roth** ** **Samuel A. Burden** *

* *Department of Electrical Engineering, University of Washington, Seattle, WA 98105 USA (e-mail:* {my13,dbhowell,sburden}@uw.edu*).*
** *Department of Intelligent Systems Engineering, Indiana University, Bloomington, IN 47405 USA (e-mail:* eatai@iu.edu*).*

Abstract:

Keywords:
Human-machine interface, sensorimotor learning, human-in-the-loop,
ER: more concise keyword list

1. INTRODUCTION

From robot-assisted surgery to (semi-)autonomous driving, systems in which control is shared between humans and artifacts—human-cyber-physical systems (HCPS)—are increasingly common. Whereas controllers in cyber-physical systems are designed (and therefore known), the emergent dynamics of the closed-loop *human*-cyber-physical system is shaped by the human operator, whose controller is not known *a priori*. Human controllers exhibit significant variability both between populations (e.g. novices and experts) and within an individual (e.g. performance may improve with experience and degrade with fatigue) (Abbink et al., 2012). As such, a predictive model of human controllers (or a particular human's controller) could provide an important tool for designing cyber-physical-systems tuned to perform robustly with a human in the loop. For example, haptic shared control has been suggested as a method to enhance driving safety when drivers and semi-autonomous cars share control (Mulder et al., 2012)

In this work, we consider a trajectory tracking task in which a human operator learns to control a novel dynamical system, a task akin to steering a vehicle or guiding a robot manipulandum. Traditionally, trajectory tracking tasks with a steady-state assumption have been used to understand how human operators control linear (or weakly nonlinear) systems. Pilot (expert) models of manual control of an aircraft demonstrated that control theory can be applied to HCPS to predict and explain the behavior of pilot-vehicle systems (McRuer and Jex, 1967; Allen and McRuer, 1979). These models are specifically designed for regulation tasks performed by experts, and may be difficult generalize to more complex dynamical systems or novices.

In addition to applying feedback control on tracking error, studies have suggested that humans use internalized dynamical representations of their bodies and the environments they interact with (Shadmehr and Mussa-Ivaldi, 1994); we hypothesize that this finding extends to the devices or vehicles they use. Importantly, such internal models permit *feedforward* control, allowing the human to predict the necessary inputs to produce the desired output trajectory, potentially increasing task performance and decreasing reliance on sensory feedback (Gawthrop et al., 2009, 2011; Desmurget and Grafton, 2000).

We experimentally investigate the human controller architecture from (Roth et al., 2017; Robinson et al., 2016) containing parallel feedback and feedforward pathways. This dynamic inverse model mathematical framework suggests that humans learn the forward model M and implement the inverse model as a feedforward controller, $F = M^{-1}$. Our novel experiment design enables straightforward estimation of the human feedback and feedforward transformations in terms of empirical frequency responses.

2. PROBLEM FORMULATION

2.1 Trajectory Tracking via Dynamic Model Inversion

In the laboratory, we instantiate the human-cyber-physical interaction as a single-degree-of-freedom, reference-tracking task: a path-following video game in which the human operator is tasked with guiding a cursor, y, along a prescribed path, r (Fig. 1b). The human participant uses a 1DOF sliding joystick to modulate the input u. The cyber-physical system dynamics are prescribed by the model, M, transforming human inputs into cursor motion.

We hypothesize that the human sensorimotor controller comprises parallel feedforward and feedback pathways, F and B respectively. The dynamic inverse model mathematical framework suggests that humans learn the forward model M and implement the inverse model as a feedforward controller, $F = M^{-1}$. Assuming perfect model learning and inversion, the feedforward controller prescribes the input trajectory that yields an output precisely matched to

⋆ This research was sponsored by .

the reference; the feedback pathway contributes nothing. In a less perfect scenario (e.g., imperfect model learning, process noise), the feedforward transform provides the nominally ideal input and the feedback pathway corrects any deviations from the reference trajectory, tracking error. For this study, we we have included a disturbance with no look ahead that forces users to use the feedback pathway to correct unforseen deviations from the nominal trajectory. (Roth et al., 2017) demonstrated that novice operators, when tasked to follow a prescribe trajectory, exhibit responses (user inputs, $u(t)$) that suggest a combination of feedforward and feedback control.

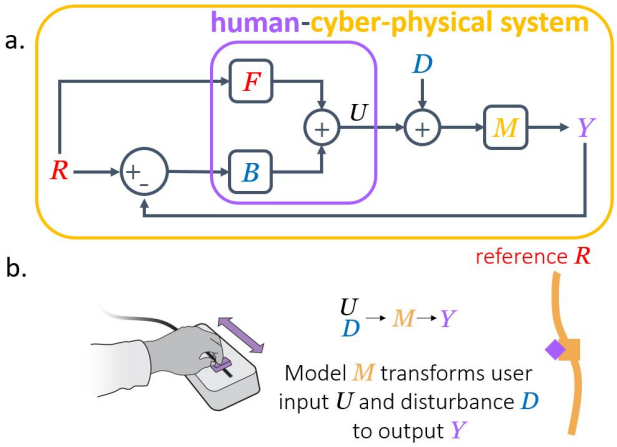

Fig. 1. a. The block diagram of HCPS highlights the feedback and feedforward human controller separation that adds to a user input U. b. A human operator completing the computer trajectory tracking task using a one-dimensional slider.

Our experimental assays prescribe the reference and disturbance signals, r and d, as well as the cyber-physical model, M, and are designed to enable estimation of the distinct contributions of feedforward and feedback processes.

Hypothesis 2.1. If the reference and disturbance is tracked simultaneously, then the input required to track both is equal to the summation of tracking only the reference and only the disturbance separately.

2.2 Separation of Feedforward and Feedback Control Inputs

Feedforward controller F and feedback controller B can be described in the frequency domain by,

$$B = \frac{-H_{DU}}{M(1+H_{DU})}, \tag{1}$$

$$F = H_{RU}(1+BM), \tag{2}$$

where H_{RU} represents the transfer function that maps r in the frequency domain R to U such that $U = H_{RU}R$, and H_{DU} is the transfer function that maps D to U such that $U = H_{DU}D$. These controllers can be obtained empirically for each frequency at which we present a reference and a disturbance to the operator by simply computing the fourier transform of U, R and D. It was obtained by representing U as a combination of F and B with prescribed (R, M, D) values as shown in Fig. 1,

$$U = \frac{F+B}{1+BM}R - \frac{BM}{1+BM}D, \tag{3}$$

$$Y = (U+D)M, \tag{4}$$

and by setting $H_{RU} = \frac{U}{R}$ and $H_{DU} = \frac{U}{D}$, the equations for F, B in Eqns. 1, 2 can be obtained.

Hypothesis 2.2. A feedback and feedforward combined controller will predict the user output better than a feedforward only controller.

3. EXPERIMENTAL METHODS

3.1 Overview of Experimental Setup

An Arduino Due in conjunction with a 10 $k\Omega$ potentiometer slider was used to implement a model M wherein the input U from the slider was transformed to the output such that $Y = MU$. A scaled and phase-shifted sum of sines was used to create the reference and disturbance trajectories, with signal frequencies at some prime multiples starting from 2 to ensure no harmonic signals (Fig. 2). The phase shifts were randomly chosen, and the magnitude of the sine wave at each frequency was equivalent to $1/f$ for the first-order system, and $1/f^2$ for the second-order system, such that the larger frequencies had a lower amplitude. Each trial lasted for 40 seconds, and data was collected at 60 Hz.

Three types of assays were presented to the operator: 1. only r, with $d = 0$, 2. only d, with $r = 0$, and 3. $r + d$, with each at alternating frequencies such that for one frequency, either $r = 0$ or $d = 0$ (Fig. 2). For 3., alternating frequencies can either be at odd or even frequencies, such that the r has frequency content at even frequencies and d has frequency content at odd freqnecies, and vice versa. The d only trials differed from the r only trials by the r trajectory having a look-ahead and past of 0.25 seconds, whereas the d trajectory had no look-ahead that the operator could use to determine an optimal input u. The phase shifts were randomized for each trial, and the three assays were presented in sequence as follows:

Table 1. Assays Presented To Human Operator

Assay	$r+d$	d	$r+d$	r	$r+d$
# Trials	2	10	2	10	10

Two models were presented sequentially to observe model inversion in a simpler first-order (FO) model and a more complex second-order (SO) model, with,

$$m_{FO} : \dot{y} = u; M_{FO} : \frac{1}{s}, \tag{5}$$

$$m_{SO} : \ddot{y} - \dot{y} = u; M_{SO} : \frac{1}{s^2 - s}. \tag{6}$$

A scaled and shifted sum of sines were chosen at prime frequencies from (2-31) 1/20 Hz for the first-order system, and 2-17 1/20 Hz for the second-order system.

3.2 Experimental Data Analysis

Seven participants were recruited to track a gold trajectory with a purple cursor on the screen using a one-dimensional

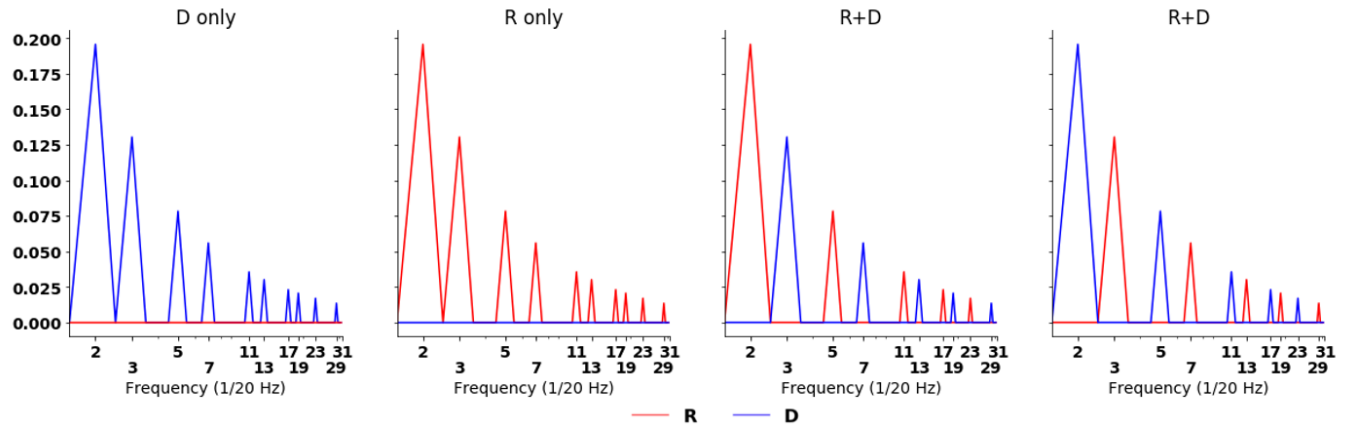

Fig. 2. The four types of assays used in the study shown as an FFT of the 40 second signal. The resolution of the axis is 0.5/20 Hz. The blue and red lines indicate frequency content for D and R respectively. Two types of alternating frequencies were prescribed - one where R had frequency content on the even primes and D on odd, and one where R had frequency content on the odd primes and D on even.

cursor (Fig. 1). Data was analyzed with Python 2.7.3 in the frequency domain by taking the fast fourier transform (FFT) of measured and known values U, M, R, D, Y for each trial, where capital letters are used to represent analysis conducted in the frequency domain. Coherence was calculated in the time domain using the python function scipy.signal.coherence() between the r, d and $r + d$ trials. H_{DU} and H_{RU} in the frequency domain were also calculated to assess linearity and superposition of the HCPS. A Wilcoxon Signed Rank test was performed to determine the extent to which the medians of H_{DU} and H_{RU} from the d, r trials are similar to the values calculated from the $r + d$ trials. The interquartile range (IQR) was calculated as a measure of spread. For all trials, circular statistics were used to unwrap the angle of the transfer functions before analyzing the data.

A feedback only model and a feedback and feedforward model was estimated using the D only and R only trials to determine whether the feedback and feedforward model had a better fit to the data than the feedback only model. The transfer functions were then applied to R and D in the $R+D$ trials which were not a part of the training data, and the percent error between the predicted U_p and measured U_o was calculated. The IQR of the error was calculated for both the feedback only model and the feedback and feedforward model.

F and B were calculated as described in Eqns. 1, 2 to determine the extent to which F was similar to the model inverse M^{-1}. A Wilcoxon Signed Rank test was performed to quantify this similarity.

4. RESULTS

4.1 Linearity of HCPS

The moderate coherence between the r and $r+d$ trials (median, range $C_{r,r+d} = 0.84, 0.21 - 1.0$) and d and $r+d$ trials (median, range $C_{d,r+d} = 0.82, 0.10 - 0.99$) demonstrated that $r + d$ trials may be well predicted from r and d trials by a linear least squares function (Fig. 4. QUANTIFY SOMETHING HERE This suggests that there may be a linear relationship between the system inputs r, u and the system output y. At the higher frequencies of 23/20, 29/20, and 31/20 Hz, there was a lower overall coherence as well as a more varied coherence than at the lower frequencies, as demonstrated by the larger deviation from the median in the 1st and 3rd quartile.

Further investigation into the transfer functions H_{RU} and H_{DU} demonstrated a high degree of overlap between the R and $R+D$ trials and D and $R+D$ trials. The Wilcoxon signed-rank test indicated that with $\alpha < 0.05$, there was no statistical difference in H_{RU} and H_{DU} in either average magnitude or angle between the only R or only D trials and the $R + D$ trials. Similarly to the coherence analysis, the higher frequencies tended to have a larger spread in variability across individuals for both the R only and D only trials as well as the $R + D$ trials. The positive results from this superposition test indicates that the HCPS can be thought of and analyzed as a linear system for lower frequencies. WHICH LOWER FREQUENCIES

4.2 Feedback and Feedforward Combined Controllers Versus Feedback Only Controller

As hypothesized in 2.2, human operators may control cyber-physical systems with a combination of feedforward and feedback control strategies. We verified that when a feedback only model was fitted to a subsection of the data (R only and D only trials) and tested on a separate set of data ($R + D$ trials), the error between the predicted U_p and observed U_o was worse than the error from the fitted feedback and feedforward model at all frequencies (Fig. 5). The error linearly increases in the log-log plot, suggesting that for the first-order model, the error is inversely proportional to the amplitude of the shown signal.

4.3 Dynamic Model Inversion

The feedback and feedforward estimates pooled across all individuals and trials demonstrate large deviations in magnitude from M^{-1} for the feedforward controller for

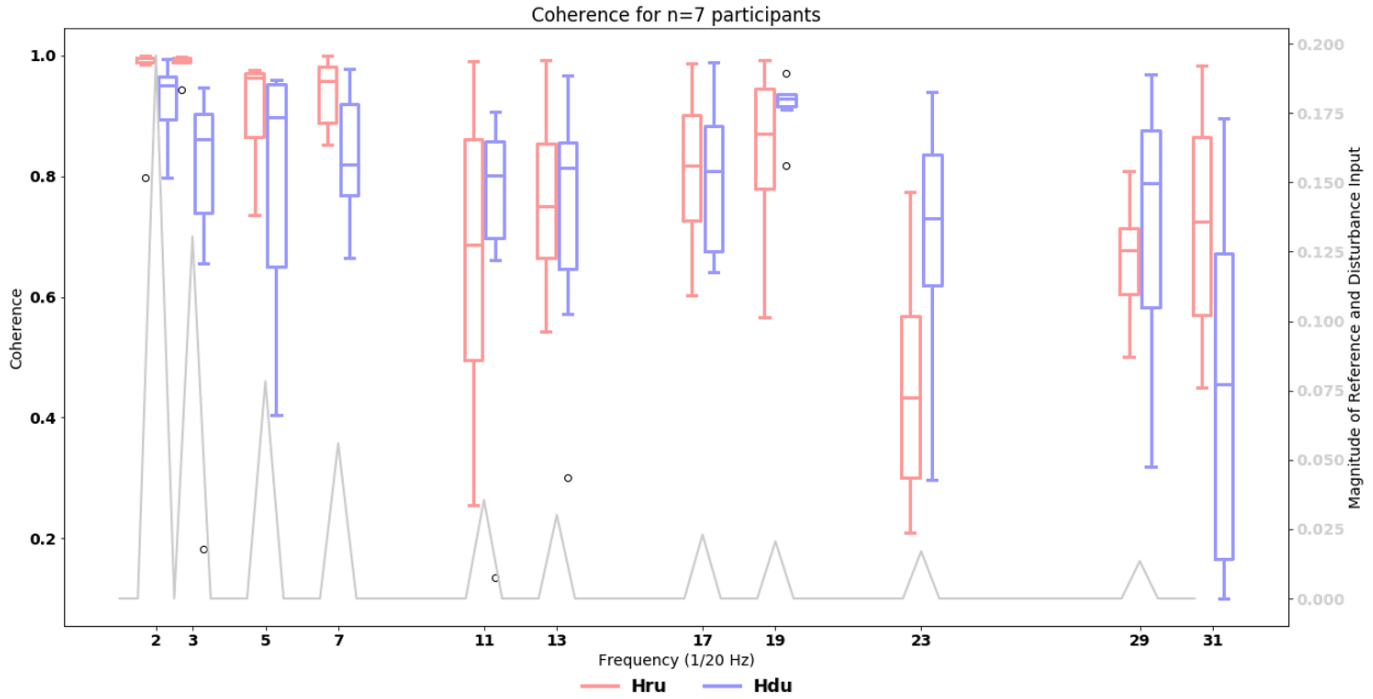

Fig. 3. Coherence values calculated between the r and d only trials and $r+d$ trials demonstrate high coherence between the two for lower frequencies, whereas the coherence at higher frequencies show a higher variability between subjects.

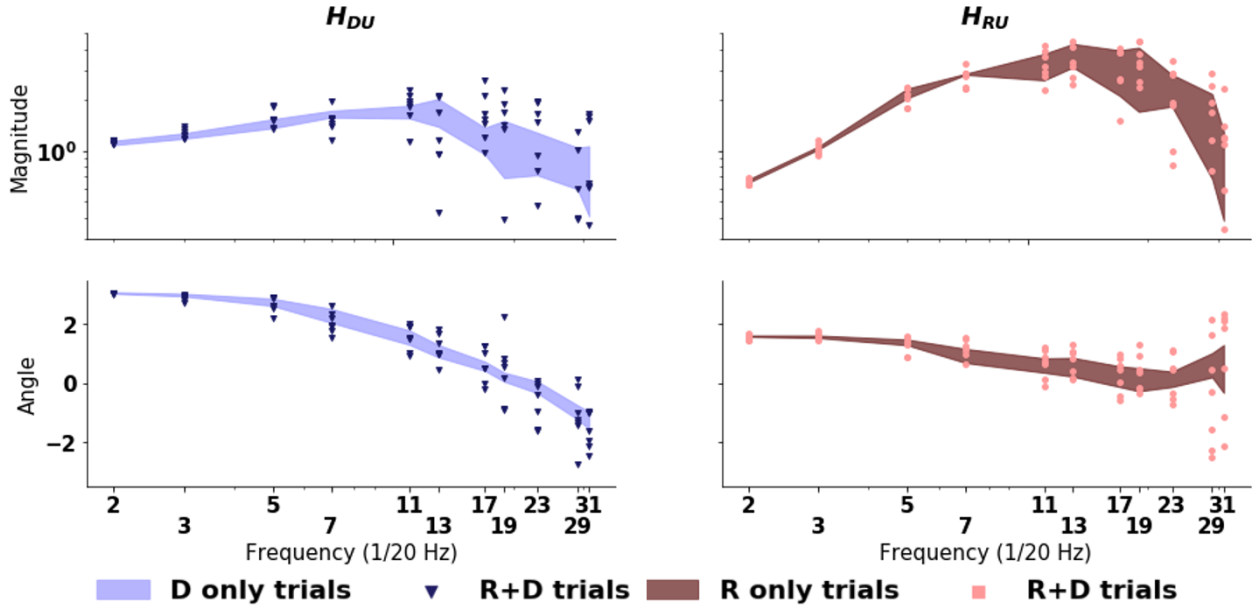

Fig. 4. Transfer functions for D to U ($H_{DU} = U/D$) and R to U $H_{RU} = U/R$ demonstrate overlap for the transfer functions in the R and D only trials and $R+D$ trials. The shaded blue and red areas represent the IQR of H_{DU} and H_{RU} respectively, the blue triangle represents individual H_{DU} values calculated from the $R+D$ trials, and the red circle represents individual H_{RU} values calculated from the $R+D$ trials.

both R and $R+D$ trials (Fig. 6). The Wilcoxon signed-rank test performed on the F_{R+D} calculated from the $R+D$ trials demonstrated that there was a significant difference between the feedforward controller and M^{-1} for the magnitudes (first-order: $p = 0.006$, second-order: $p = 0.018$). The angle of the experimental feedforward block was significantly different from M^{-1} for the first order M ($p = 0.004$), but not for the second order (p=0.18). Similarly, for the F calculated from the R only and D only trials, there was a significant difference in the magnitudes between the $F_{R,D}$ and M^{-1} (first-order: $p = 0.004$, second-order: $p = 0.04$) and the angle for the first-order model (p=0.006), while we again failed to verify a difference in the angles for the second-order system (p=0.74).

For both the first and second order model, the magnitude was consistently lower than the expected M^{-1} at all

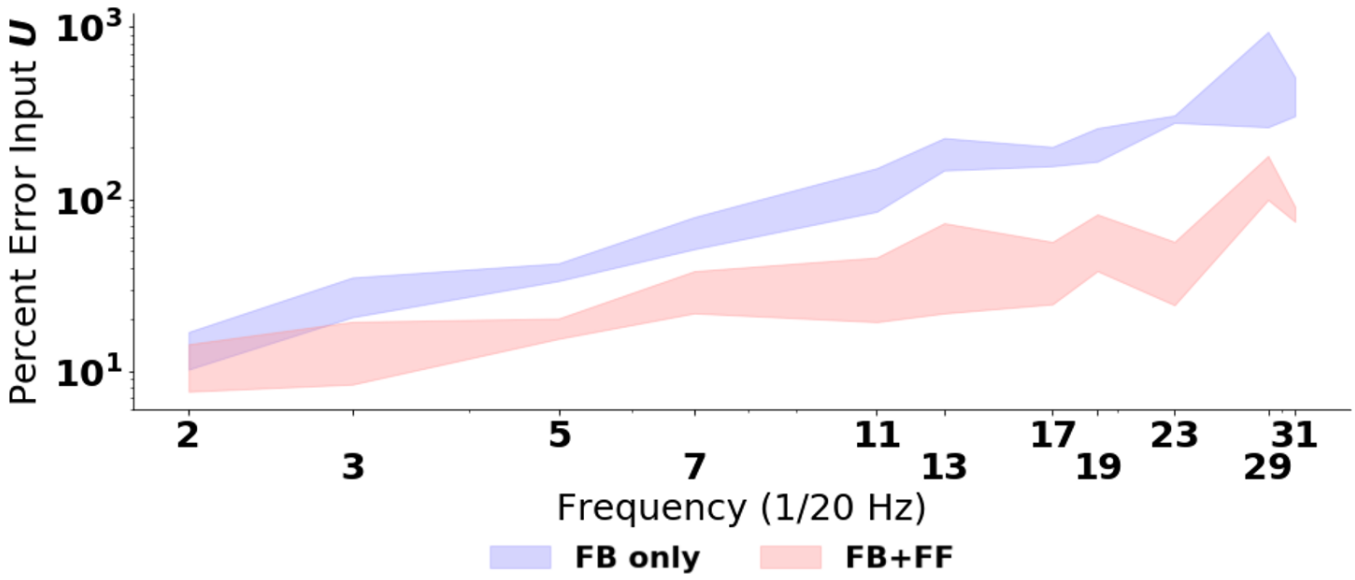

Fig. 5. The percent error between the predicted input and actual user input for the feedback only model (blue shaded area) and feedback and feedforward model (red shaded area) demonstrates lower percent error at all frequencies for the feedback and feedforward model.

frequencies except $2/20Hz$. BY WHAT FACTOR WAS IT LOWER

5. MOMONA'S DISCUSSION

We estimated feedback and feedforward elements of human sensorimotor control in a trajectory tracking task. Estimates were obtained for two models ($1/S$ and $1/(S^2 - S)$) using two different assays; both estimates agreed to within experimental error for frequencies up to 3/20 Hz. Furthermore, including the feedforward pathway roughly halves the human input prediction error, suggesting both feedforward and feedback elements are needed to predict human control of cyber–physical systems.

In contrast to the recent results reported in (Zhang et al., 2018), the estimated feedforward transformation only agrees with the inverse of the cyber–physical system model at low frequencies. At higher frequencies we demonstrated that the magnitudes are lower than the expected magnitude of M^{-1} (Fig. 6). This was corroborated with our statistical tests, which demonstrated that with an $\alpha < 0.05$, the median for both models did not have M^{-1} for the mean for either the magnitude or the angle.

This result is congruent with the coherence values calculated in Fig. 3, which demonstrated that lower frequencies tended to have a higher median coherence and smaller variability than the higher frequencies. The transfer functions for H_{DU} and H_{RU} had similar results where frequencies larger than 11/20 Hz tended to have a much larger variability in both magnitude and angle than the lower frequencies.

This may be due to a number of reasons, including the strength of the signal provided and the limits of the human visuomotor system. For this study, we chose to provide human operators with a lower signal amplitude for higher frequencies inversely proportional to the frequency for first-order, and inversely proportional to the square of the frequency for the second-order system, which will magnify any errors that the human operator makes while tracking these higher frequencies. Another possible explanation is human visuomotor limitations which suggests that the fastest motor reaction time for humans (as demonstrated by asking a human subject to press a button upon the presentation of a certain visual) is about 5 Hz.

The increasing error with frequency from fitting a model to the data assuming only feedback control versus assuming a combination of feedback and feedforward control also demonstrates that the lower signal amplitude at higher frequencies affect the signal quality. While the feedback and feedforward model can do no worse than the feedback only model in predicting the output of the training dataset, the increased number of variables in the feedback and feedforward model may lead to overfitting to the training dataset. We found that by testing our fitted model on a testing dataset however, that this was not the case, and the combined feedback and feedforward model had less error at all frequencies when predicting the U compared to the feedback only model.

6. CONCLUSION

This paper proposes a novel experiment design that enables estimation of human feedback and feedforward transformations in trajectory tracking tasks directly from empirical frequency responses to reference and disturbance inputs. Our findings provide support for the hypothesis that humans utilize internalized dynamical representations of cyber-physical systems under their control. Our results do not support the hypothesis that humans learn to use the inverse of the cyber-physical system model in their feedforward control pathway, although the estimated feedforward transformation resembles a scaled-down version of the model inverse. Further investigations are needed to

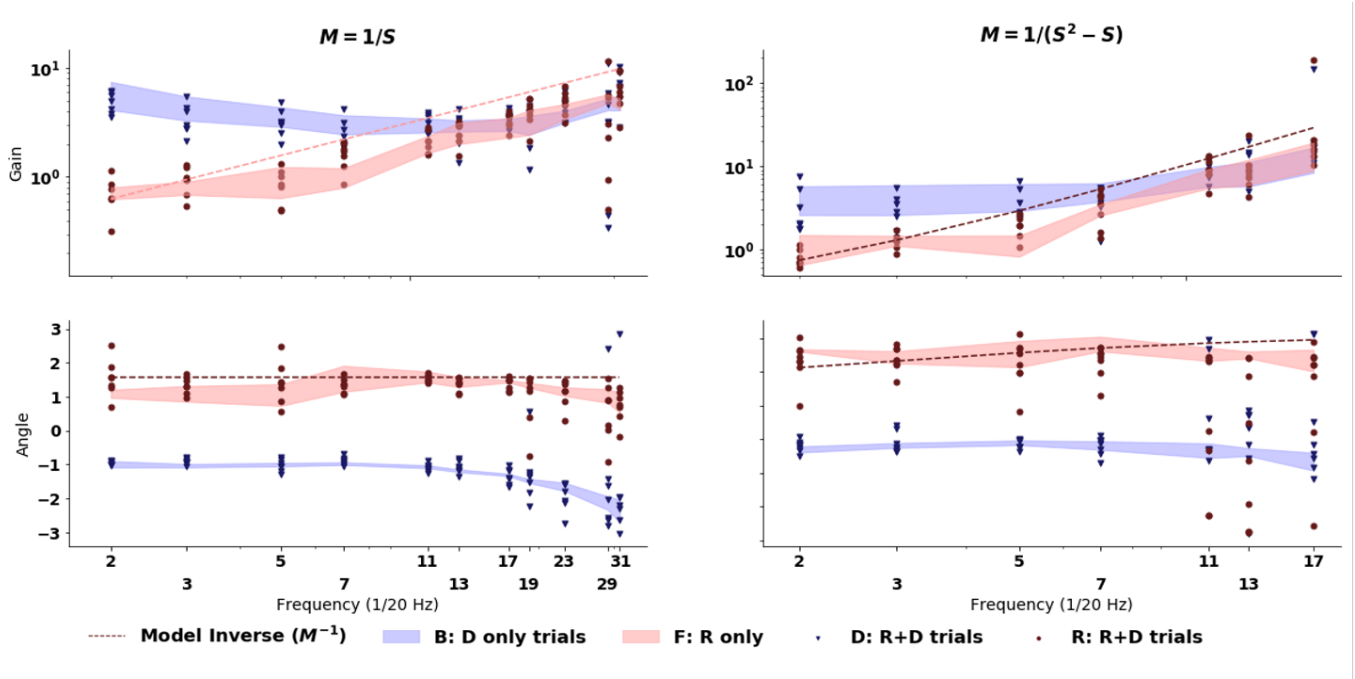

Fig. 6. The experimental values of F and B demonstrate for both first and second order closer model inversion for lower frequencies than higher frequencies in magnitude. The red dotted line represents the model inverse, the shaded red and blue is the IQR for F and B calculated from R only and D only trials, and the dark blue triangle and dark red circle represents F and B calculated from $R + D$ trials for each individual. For higher frequencies, the magnitude is consistently lower than the expected magnitude from M^{-1}

.

characterize the feedforward transformations learned by human operators.

ACKNOWLEDGEMENTS

This research is supported by a grant from the National Science Foundation under the CISE CRII CPS (Award # 1565529), the Air Force Office of Scientific Research under grant FA9550-14-1-0398, and the Washington Research Foundation Funds for Innovation in Neuroengineering.

REFERENCES

Abbink, D.A., Mulder, M., and Boer, E.R. (2012). Haptic shared control: smoothly shifting control authority? *Cognition, Technology & Work*, 14(1), 19–28.

Allen, R.W. and McRuer, D. (1979). The man/machine control interfacepursuit control. *Automatica*, 15(6), 683–686.

Desmurget, M. and Grafton, S. (2000). Forward modeling allows feedback control for fast reaching movements. *Trends in cognitive sciences*, 4(11), 423–431.

Gawthrop, P., Loram, I., and Lakie, M. (2009). Predictive feedback in human simulated pendulum balancing. *Biological cybernetics*, 101(2), 131–146.

Gawthrop, P., Loram, I., Lakie, M., and Gollee, H. (2011). Intermittent control: a computational theory of human control. *Biological cybernetics*, 104(1-2), 31–51.

McRuer, D.T. and Jex, H.R. (1967). A review of quasi-linear pilot models. *IEEE Transactions on Human Factors in Electronics*, (3), 231–249.

Mulder, M., Abbink, D.A., and Boer, E.R. (2012). Sharing control with haptics: Seamless driver support from manual to automatic control. *Human factors*, 54(5), 786–798.

Robinson, R.M., Scobee, D.R., Burden, S.A., and Sastry, S.S. (2016). Dynamic inverse models in human-cyber-physical systems. In *Micro-and Nanotechnology Sensors, Systems, and Applications VIII*, volume 9836, 98361X. International Society for Optics and Photonics.

Roth, E., Howell, D., Beckwith, C., and Burden, S.A. (2017). Toward experimental validation of a model for human sensorimotor learning and control in teleoperation. In *Micro-and Nanotechnology Sensors, Systems, and Applications IX*, volume 10194, 101941X. International Society for Optics and Photonics.

Shadmehr, R. and Mussa-Ivaldi, F.A. (1994). Adaptive representation of dynamics during learning of a motor task. *Journal of Neuroscience*, 14(5), 3208–3224.

Zhang, X., Wang, S., Hoagg, J.B., and Seigler, T.M. (2018). The roles of feedback and feedforward as humans learn to control unknown dynamic systems. *IEEE transactions on cybernetics*, 48(2), 543–555.